Push-Pull-Pull Interactions of 2D Imide-Imine based Covalent Organic Framework to Promote Charge Separation in Photocatalytic Hydrogen Production

Islam M. A. Mekhemer [a,b#], Mohamed M. Elsenety[c,a#], Ahmed M. Elewa[a], Khanh Do Gia Huynh[a], Maha Mohamed Samy[b,d], Mohamed Gamal Mohamed[b,d], Dalia M. Dorrah[a], Dung Chau Kim Hoang[a], Ahmed Fouad Musa[a], Shiao-Wei Kuo[d], and Ho-Hsiu Chou[a,e, f*]

[a]Department of Chemical Engineering, National Tsing Hua University, Hsinchu 300044, Taiwan.

[b]Chemistry Department, Faculty of Science, Assiut University, Assiut, 71515, Egypt.

[c]Chemistry Department, Faculty of Science, Al-Azhar University, Cairo, 11884, Egypt.

[d]Department of Materials and Optoelectronic Science, Center of Crystal Research, National Sun Yat-Sen University, Kaohsiung 804, Taiwan.

[e]College of Semiconductor Research, National Tsing Hua University, Hsinchu 300044, Taiwan.

[f]Photonics Research Center, National Tsing Hua University, Hsinchu 300044, Taiwan.

[*] Corresponding author: E-mail: hhchou@mx.nthu.edu.tw (H.H. Chou)

[#] Equal contribution

1. Materials and Methods

Anhydrous potassium carbonate, 1,2,4,5-tetrabromobenzene, (4-formyl phenyl) boronic acid, 1,3,6,8-tetrabromopyrene, tetrakis(triphenylphosphine)palladium(0), and silica gel for column chromatography were purchased from commercial sources. All organic solvents such as methanol, tetrahydrofuran (THF), acetone, nitrobenzene, mesitylene, p-dioxane, trifluoroacetic acid, and dichloromethane (DCM) were analytical grade reagents used without further purification.

2. Characterization

FTIR spectra were collected on a Bruker Tensor 27 FTIR spectrophotometer with a resolution of 4 cm^{-1} by using the KBr disk method. ^{13}C nuclear magnetic resonance (NMR) spectra were examined using an INOVA 500 instrument with DMSO and $CDCl_3$ as the solvent and TMS as the external standard. Chemical shifts are reported in parts per million (ppm). The thermal stabilities of the samples were performed by using a TG Q-50 thermogravimetric analyzer under an N_2 atmosphere; the cured sample (ca. 5 mg) was put in a Pt a cell with a heating rate of 20 °C min^{-1} from 100 to 800 °C under an N_2 flow rate of 60 mL min^{-1}. Wide-angle X-ray diffraction (WAXD) patterns were measured by the wiggler beamline BL17A1 of the National Synchrotron Radiation Research Center (NSRRC), Taiwan. The morphologies of the polymer samples were examined by Field emission scanning electron microscopy (FE-SEM; JEOL JSM7610F) and by transmission electron microscope (TEM) using the JEOL-2100 instrument at an accelerating voltage of 200 kV. BET surface area and porosimetry measurements of samples (ca. 40–100 mg) were measured using BEL Master™/BEL sim™ (v. 3.0.0). N_2 adsorption and desorption isotherms were generated through incremental exposure to ultrahigh-purity N_2 (up to ca. 1 atm) in a liquid N_2 (77 K) bath. Surface parameters were calculated using BET adsorption models in the instrument's software. The prepared samples' pore size was determined using nonlocal density functional theory (NLDFT). We recorded the photoluminescence (PL) conductance of the COF-based imide-imine linkage from the fluorescence emission spectra of their corresponding solutions via Hitachi 11 F-7000 spectrophotometer equipped with a

Xenon lamp (λ = 250 ~ 800 nm), We dissolved these COFs in N-methyl pyrrolidine at 1 mg mL^{-1}, as the limiting concentration, followed by excitation with light at 350 nm. Ultraviolet/visible diffuse reflectance spectroscopy (UV–Vis DRS) of synthesized COPs were detected via a Hitachi U-3300 spectrophotometer. Electrochemical Impedance Spectroscopy (EIS) was performed on a Zahner Zennium E workstation equipped with a three-electrode cell including a Pt wire counter electrode, Ag/AgCl as reference electrode (3M NaCl), and a fluorine-doped tin oxide (FTO) glass as working electrode. About 5 mg of COFs were dispersed into an acetonitrile solution (1 mL) with 30 μL Nifion and sonicate for 1 h. After that, 200 μL of as-prepared suspension was spin-coated on FTO glass with an active area of 6.875 cm^2. Here, 0.5 M Na_2SO_4 aqueous solution was prepared as an electrolyte. 1.5 V constant potential was applied under LED light irradiation (300 W/cm^2). The COF photocatalysts time-resolved photoluminescence (TRPL) spectra were measured on a spectrometer (FLS980, Edinburgh Instruments) with a gated photomultiplier tube. The energy levels of the HOMO were measured using a photoelectron spectrometer (model AC-2). The energy levels of the LUMOs were calculated by subtracting the Eg from the HOMO energy levels.

3. Synthetic Procedures of Monomers

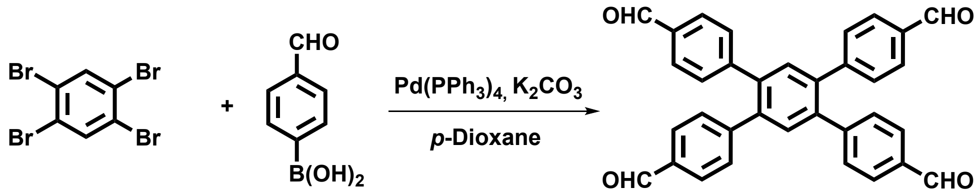

Scheme S1: 1,2,4,5-Tetrakis-(4-formylphenyl)benzene (TFPB-4CHO).

TFPB-4CHO was prepared according to the reported method with some modifications[1]. We added 1,2,4,5-Tetrabromobenzene (1.5g, 3.033 mmol), 4-formylphenylboronic acid (3.638g, 24.264 mmol), palladium tetrakis(triphenylphosphine) (0.175 g, 0.15 mmol, 5 mol%), and anhydrous potassium carbonate (6.716 g, 48.520 mmol) in *p*-Dioxane (50 mL) in the sealed tube (250 mL) and then degassed under argon for 20 minutes and heated the mixture for 72 h at 120 °C. The suspension reaction mixture was poured into slurry ice containing 60 mL of concentrated hydrochloric acid to neutralize the excess potassium carbonate. The solid product was filtered and washed thrice with water and 2 M HCl. The crude product was purified using short-column chromatography with dichloromethane as eluent. The DCM was evaporated under reduced pressure to obtain the final product as a yellowish powder (1.7 g, 90.4%). FTIR (KBr, cm^{-1}; 3038 (CH aromatic), 2827, 2740 (H<u>C</u>=O), 1699 (C=O), 1606 and 1576 (C=C) (**Figure 2a)**; ^{1}H NMR (500 MHz, $CDCl_3$) δ 9.98 (s, 4H, CHO), 7.77 (d, J = 8.1 Hz, 8H), 7.58 (s, 2H), 7.37 (d, J = 8.1 Hz, 8H) (**Figure S1)**; ^{13}C NMR (126 MHz, $CDCl_3$) δ 191.64, 146.07, 139.72, 135.32, 132.82, 130.43, 12 9.70 (**Figure S2)**; Anal. Calcd for $C_{34}H_{22}O_4$: C, 82.58; H, 4.48; O, 12.94%. Found: C, 82.40; H, 4.42; O, 12.97%.

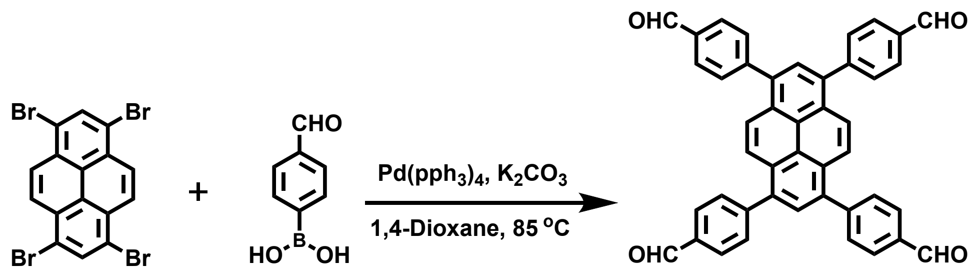

Scheme S2: Synthesis of 1,3,6,8-Tetra(4-formylphenyl)pyrene (PyTP-4CHO).

PyTP-4CHO was prepared according to the reported method with some modifications[2]. A mixture of Py-4Br (0.54 g, 1.1 mmol), $Pd(PPh_3)_4$ (0.06 g, 0.05 mmol), 4-formylphenylboronic acid (0.98 g, 6.53 mmol), and K_2CO_3 (2.30 g, 16.64 mmol) was degassed under vacuum. Dioxane (50 mL) was added, and then the mixture was heated at 85 °C for three days. The contents were poured onto ice-cold H_2O and neutralized with HCl (2 mL) to dissolve any remaining K_2CO_3. The precipitate was filtered off, washed with MeOH, recrystallized from 1,4-dioxane, and dried to produce a yellow powder (85%). FTIR (KBr, cm^{-1}, 3041 (CH aromatic), 2813, 2727 (H<u>C</u>=O), 1693 (C=O), 1606 (C=C) (**Figure 2b**). ^{1}H NMR (500 MHz, $CDCl_3$) δ 10.14 (s, 4H, CHO), 8.15 (s, 4H), 8.07 (d, J = 8.0 Hz, 8H), 8.02 (s, 2H), 7.84 (d, J = 8.0 Hz, 8H) (**Figure S3**). ^{13}CNMR result of **PyTP-4CHO** cannot be provided due to its poor solubility; Anal. Calcd for $C_{44}H_{26}O_4$: C, 85.42; H, 4.24; O, 10.34 %. Found: C, 85.67; H, 4.18; O, 11.02 %.

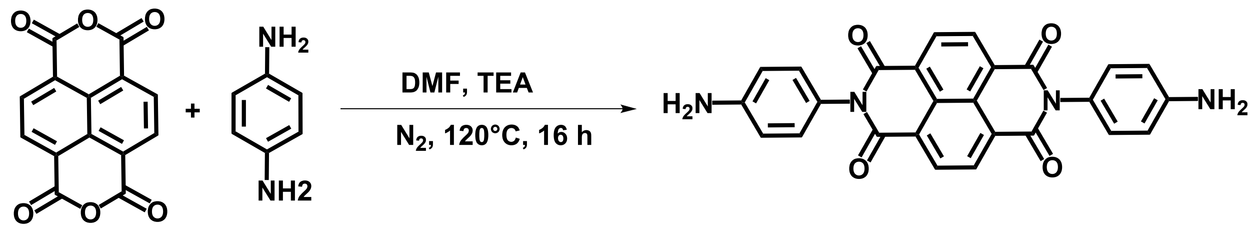

Scheme S3: Preparation of Naphthalenediimide diamine (DNI-2NH_2)

DNI-2NH_2 was prepared according to the reported method with some modifications[3]. To a round bottom flask equipped with a stir bar and condenser was added the naphthaleneanhydride (750 mg, 2.8 mmol) and diaminobenzene (3.02 g, 28.0 mmol) under inert conditions. The solids were dissolved in 50 mL of anhydrous DMF. Triethylamine (2.6 mL, 18.7 mmol) was added, and the reaction was heated to reflux for 20h. The reaction was cooled, filtered and the resulting mixture was filtered, and the residue was washed with copious amounts of water, acetone and then chloroform. The brownish red solid was isolated pure in a 95% yield. ^{1}H NMR (500 MHz, DMSO-d_6) δ 8.68 (s, 4H), 7.00 (d, J = 8.4 Hz, 4H), 6.65 (d, J = 8.4 Hz, 4H), 5.29 (s, 4H) (**Figure S4**).

4. Synthetic Procedures of COFs

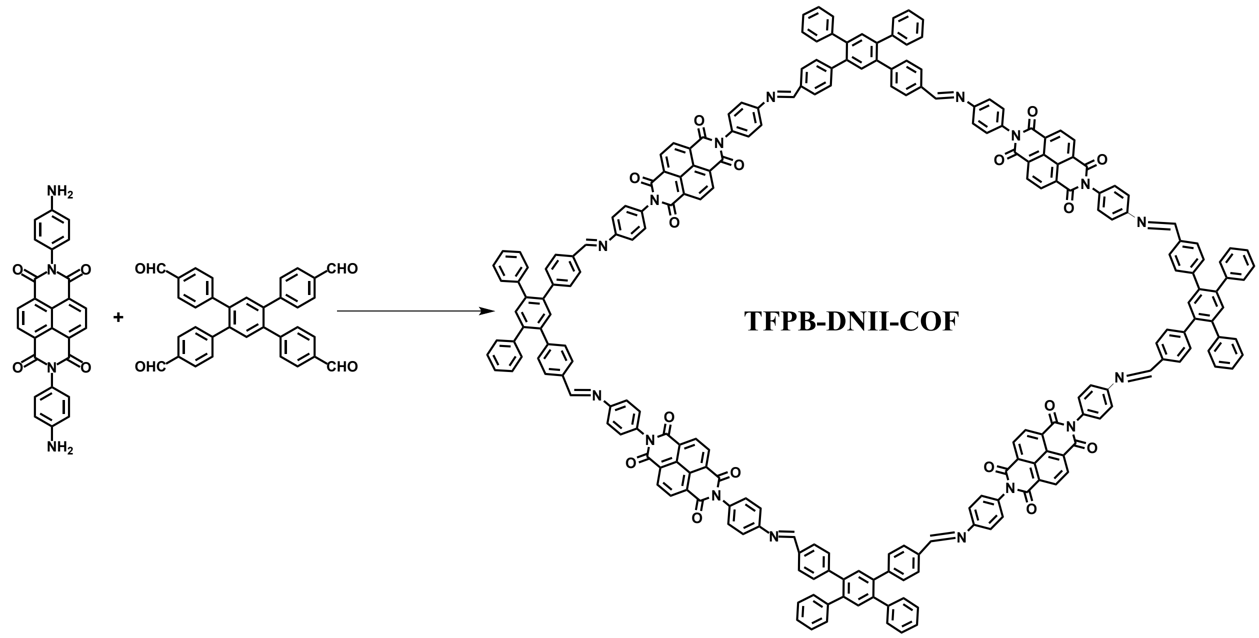

Scheme S4: Synthesis of TFPB-DNII-COF.

A 10 mL heavy-walled sealed tube was filled with 1,2,4,5-Tetrakis-(4-formylphenyl)benzene (TFPB-4CHO) (11.03 mg, 0.022 mmol), Naphthalenediimide diamine (DNI-$2NH_2$) (20.00 mg, 0.044 mmol), 1.00 mL of nitrobenzene, and 1.00 mL of mesitylene. The reaction mixture was sonicated for 5 minutes, then 10 μL of trifluoroacetic acid (TFA) was added, followed by another 10 minutes of sonication. The tube was plunged into liquid nitrogen, flash-frozen at 77 K, and evacuated to an internal pressure of 100 mTorr. The reaction was then heated to 120 °C for 4 days, resulting in the precipitation of COFs. The solid was isolated by filtration and thoroughly washed with acetone, THF, methanol, and ether. Subsequently, it was subjected to overnight Soxhlet extraction with methanol. Finally, the activated TFPB-DNII-COF was obtained by oven vacuum activation at 80 °C for 8 h.

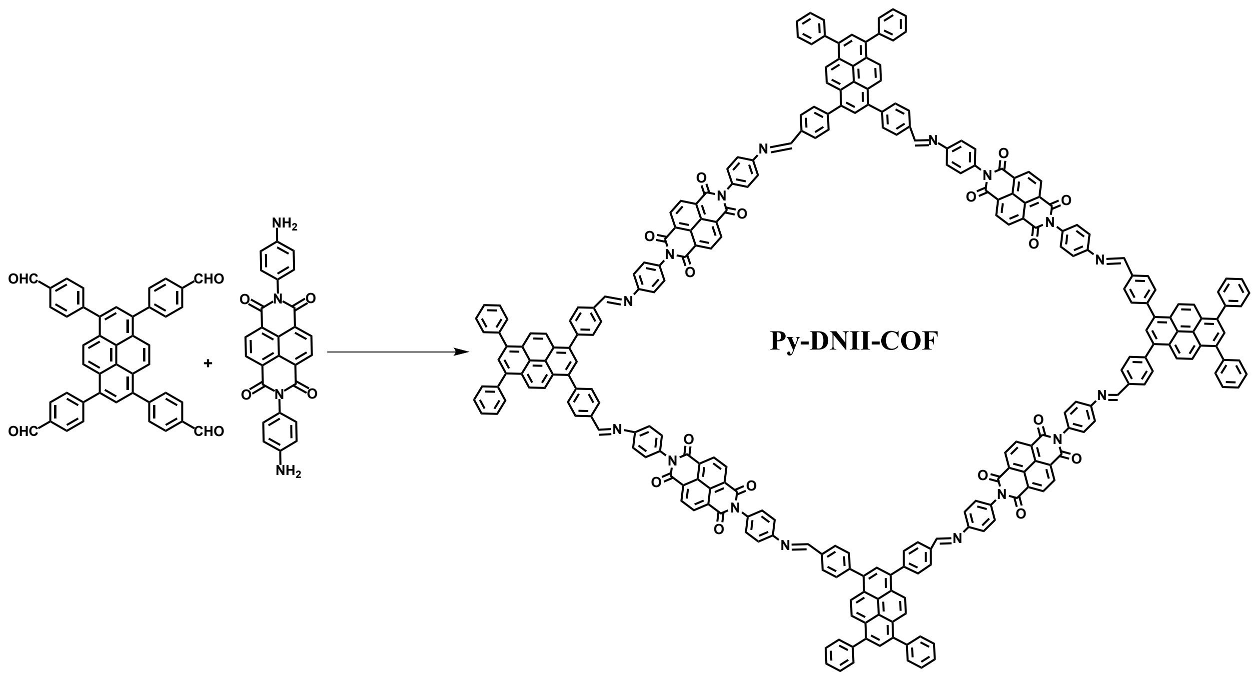

Scheme S4: Synthesis of Py-DNII-COF.

A 10 mL heavy-walled sealed tube was filled with 1,3,6,8-Tetra(4-formylphenyl)pyrene (PyTP-4CHO) (13.79 mg, 0.022 mmol), Naphthalenediimide diamine (DNI-2NH_2) (20.00 mg, 0.044 mmol), 1.00 mL of nitrobenzene, and 1.00 mL of mesitylene. The reaction mixture was sonicated for 5 minutes, then 10 μL of trifluoroacetic acid (TFA) was added, followed by another 10 minutes sonication. The tube was plunged into liquid nitrogen, flash-frozen at 77 K, and evacuated to an internal pressure of 100 mTorr. The reaction was then heated to 120 °C for 4 days, resulting in the precipitation of COFs. The solid was isolated by filtration and thoroughly washed with acetone, THF, methanol, and ether. Subsequently, it was subjected to overnight Soxhlet extraction with methanol. Finally, the activated Py-DNII-COF were obtained by oven vacuum activation at 80 °C for 8 h.

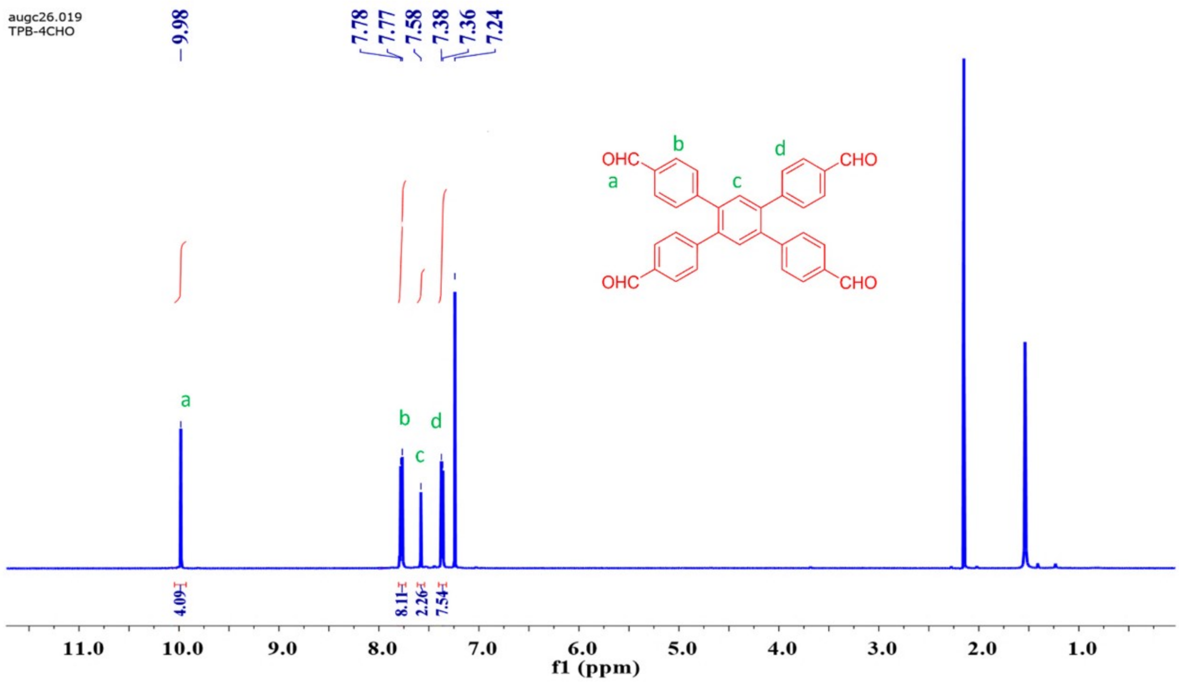

Figure S1: ^{1}H NMR of TFPB-4CHO in $CDCl_3$

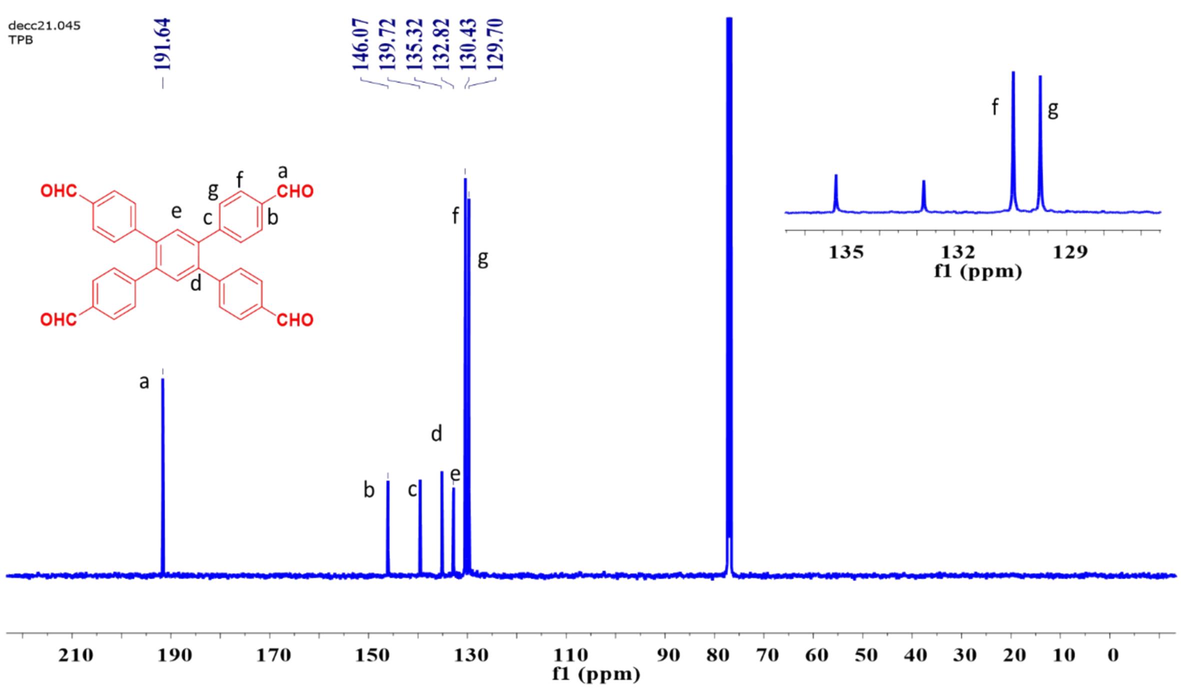

Figure S2: ^{13}C NMR of TFPB-4CHO in $CDCl_3$.

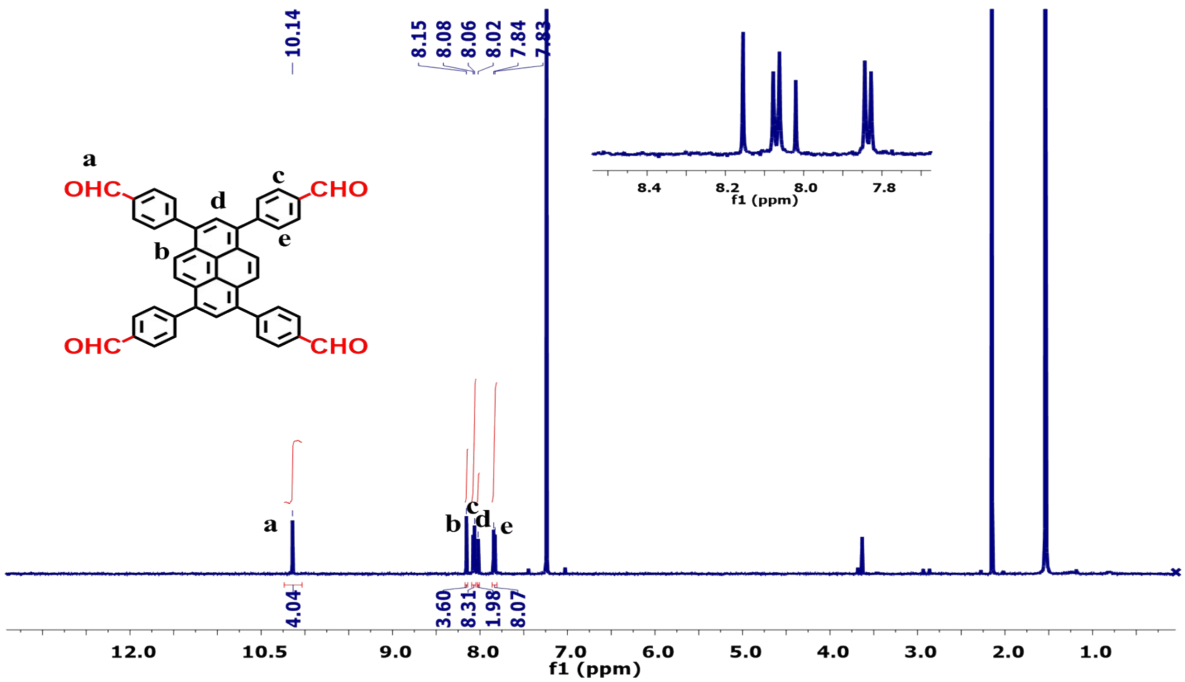

Figure S3: ^{1}H NMR of PyTP-4CHO in $CDCl_3$.

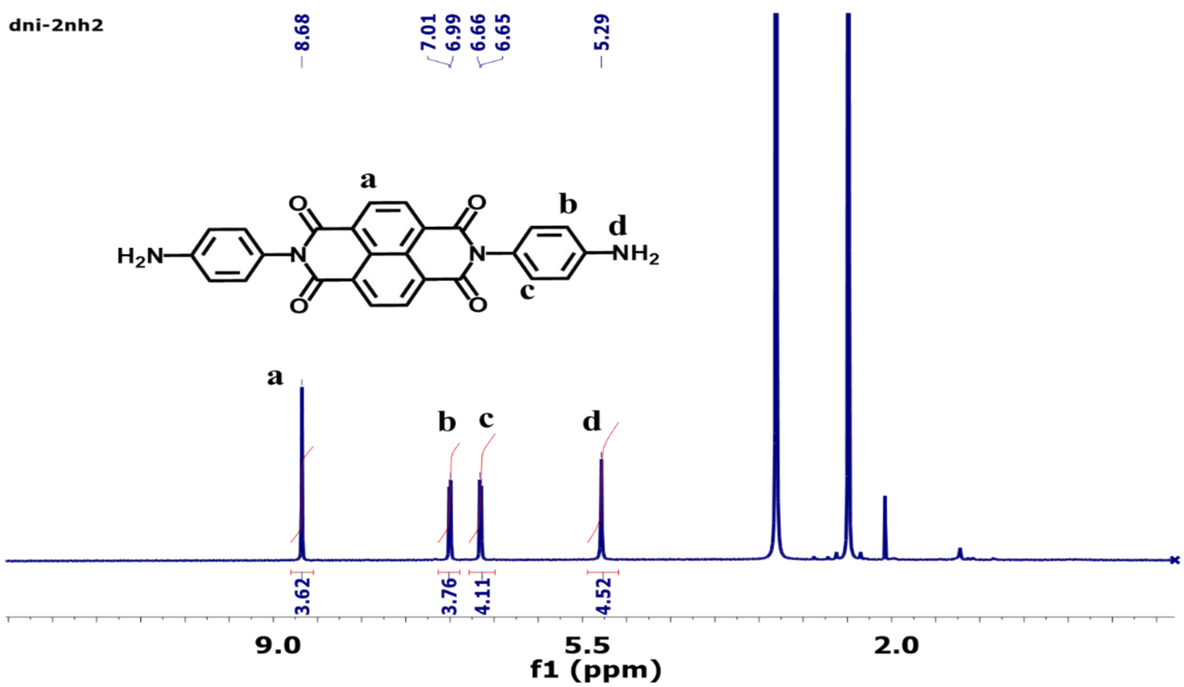

Figure S4: ^{1}H NMR for DNI-$2NH_2$.

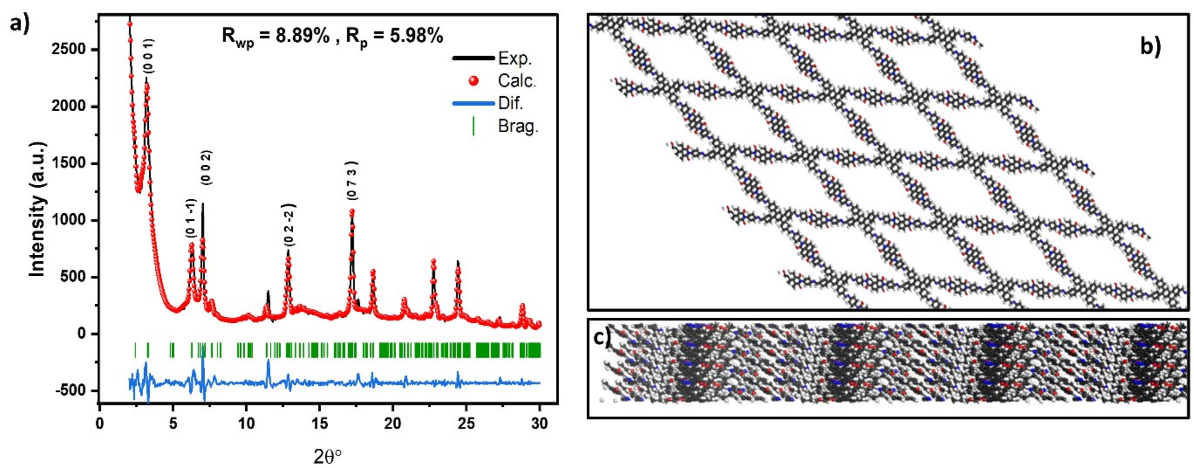

Figure S5: a) Indexed PXRD pattern of the activated sample of TFPB-DNII-COF (black) and the Pawley fitting (red) from the modeled structure, b) Simulated model for TFPB-DNII-COF (Top view), c) and side view of AA stacking.

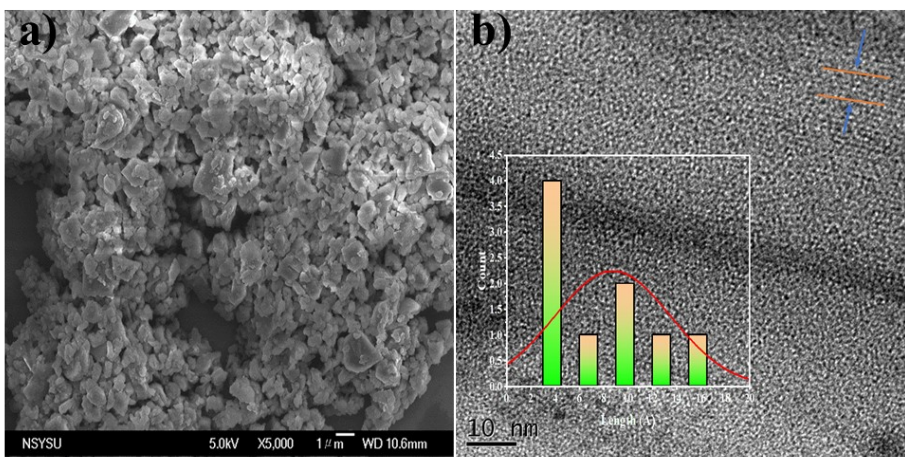

Figure S6: a) SEM and b) TEM images of TFPB-DNII-COF with lattice strip parameters.

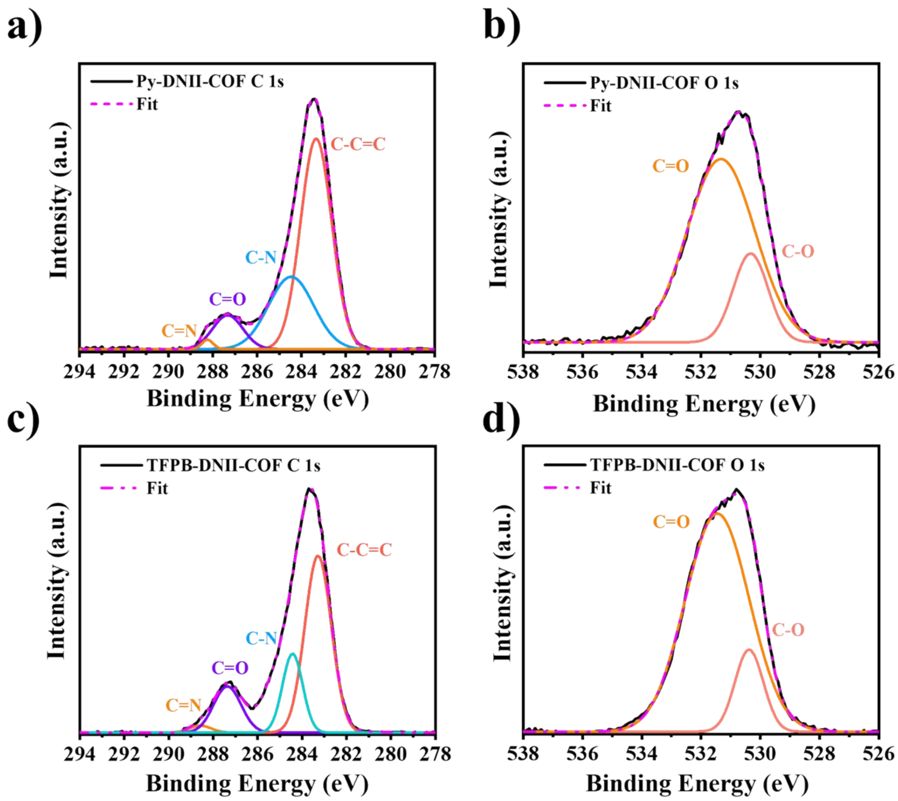

Figure S7: a-d) Core-level deconvolution spectra of C 1s and O 1s for both Py-DNII and TFPB-DNII COFs.

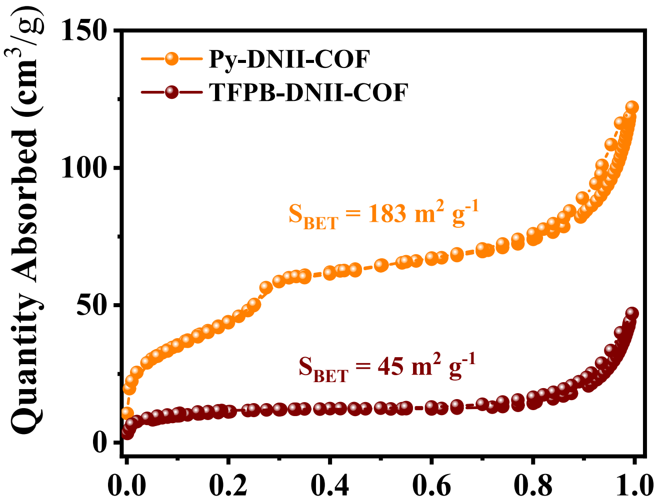

Figure S8: Nitrogen adsorption and desorption isotherms of Py-DNII-COF and TFPB-DNII-COF recorded at 77° K.

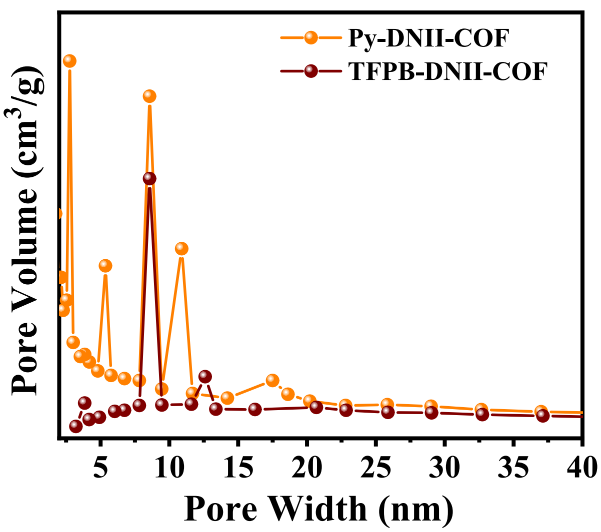

Figure S9: Pore size distribution curves of Py-DNII-COF and TFPB-DNII-COF.

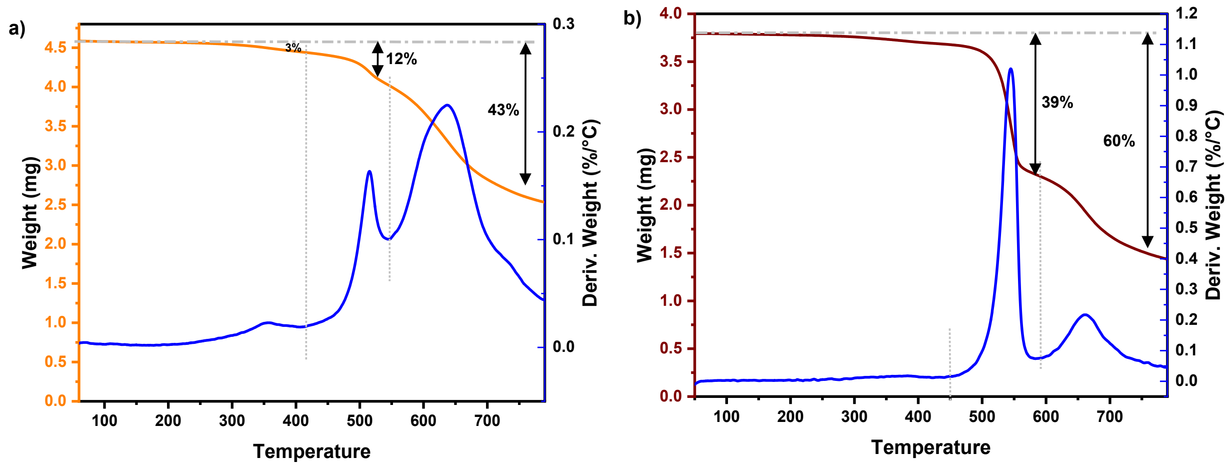

Figure S10: Thermogravimetric analysis of Py-DNII-COF (a), and TFPB-DNII-COF (b).

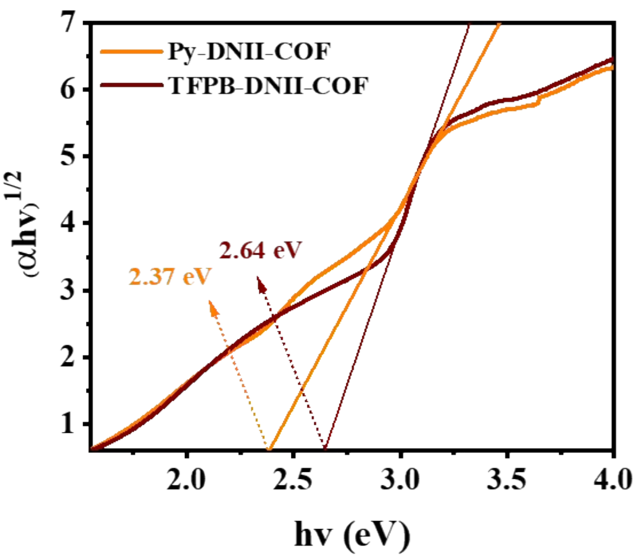

Figure S11: Tauc plot for both COFs.

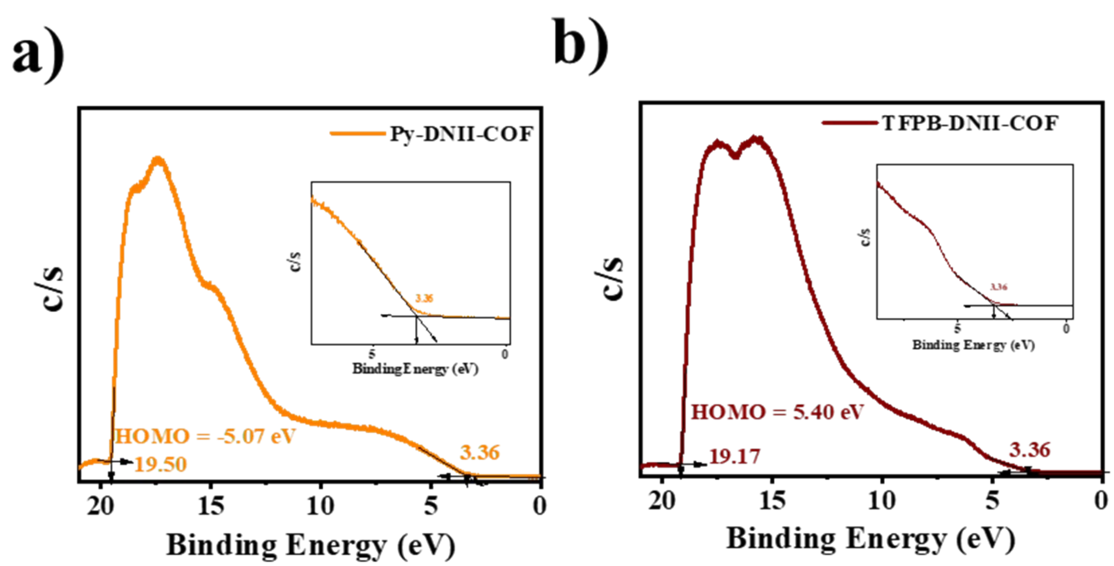

Figure S12: Ultraviolet photoemission spectroscopy (UPS) measurement of a) Py-DNII-COF and b) TFPB-DNII-COF.

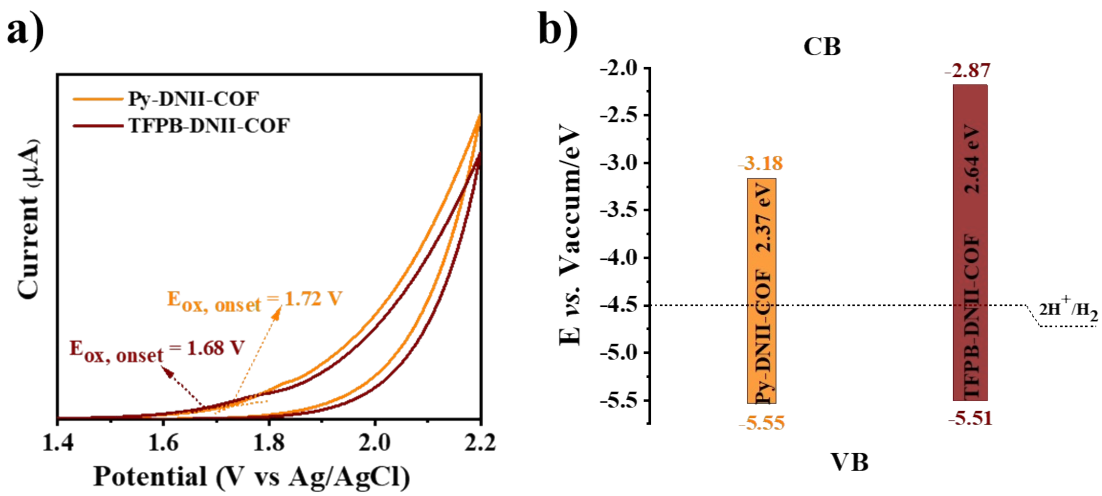

Figure S13: a) onset potential of the first oxidation peak of Cyclic voltammetry for imide-imine based COFs using Ag/AgCl as a reference electrode based on the following equation (E-HOMO = $E_{ox, onset}$-E_{Ref}+4.4) eV, E_{Ref} = 0.159+0.059*pH)**, b)** inset of schematic energy levels diagram.

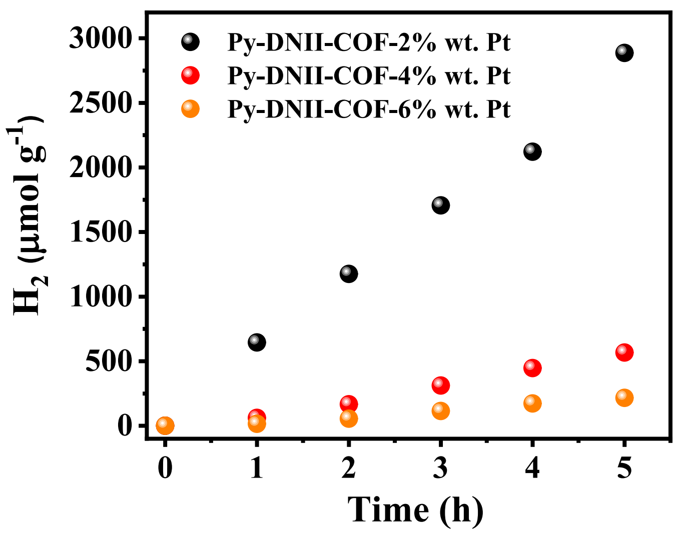

Figure S14: Time dependent HER of Py-DNII-COF photocatalysts under 380–780 nm irradiation (1.00 mg of COF powder and 10 mL of a mixed solution consisting of 80 vol.% H_2O, 20 vol.% NMP, 0.1 M of AA as SED, and 2, 4, and 6 wt% Pt as co-catalyst, respectively).

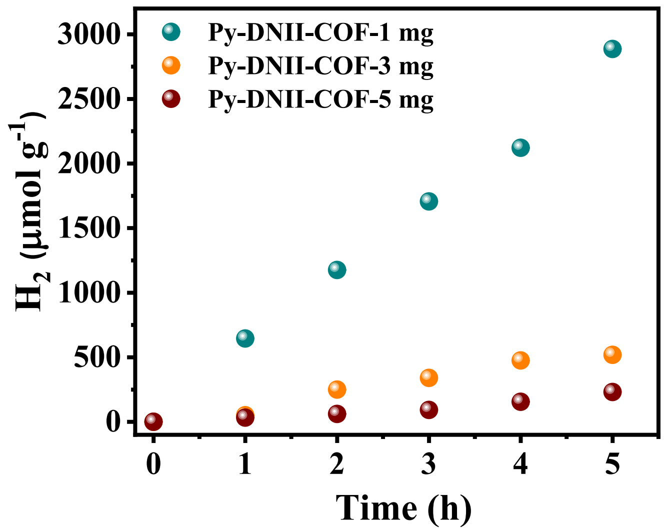

Figure S15: Time dependent HER of Py-DNII-COF photocatalysts under 380–780 nm irradiation (1, 3 and 5 mg of COF powder and 10 mL of a mixed solution consisting of 80 vol.% H_2O, 20 vol.% NMP, 0.1 M of AA as SED, and 2 wt% Pt as co-catalyst).

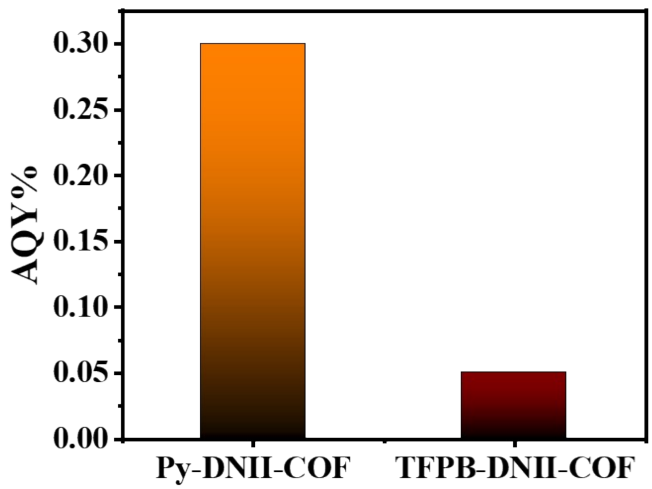

Figure S16: AQY % of imide-imine based COFs.

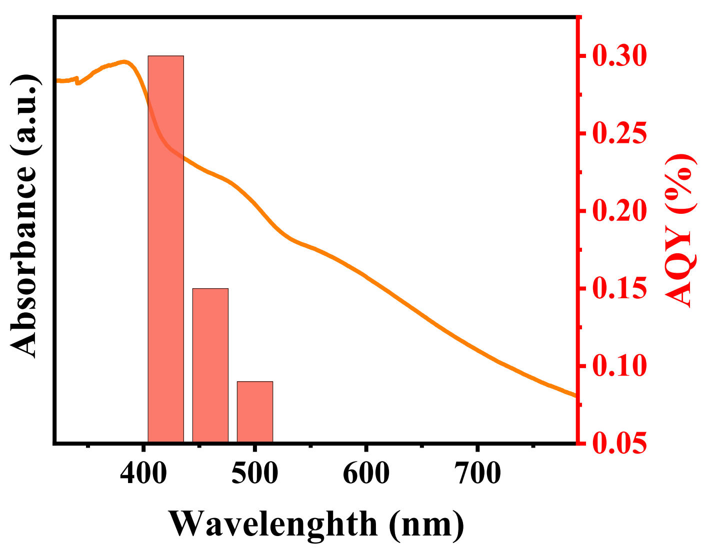

Figure S17: Correlation between the apparent quantum yield (AQY) and the UV-vis absorption spectra of Py-DNII-COF.

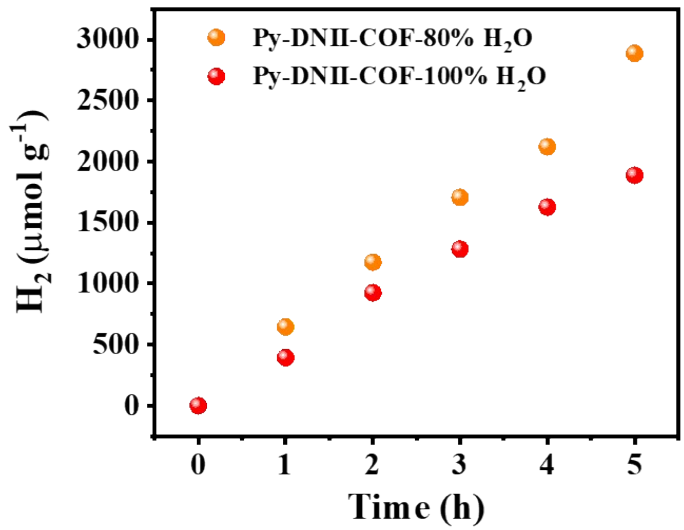

Figure S18: HER of Py-DNII-COF in the presence and absence of co-solvent (NMP).

Table S1: Atomic parameters of Py-DNII-COF

Atom	Ox.	Wyck.	Site	S.O.F.	x/a	y/b	z/c	U [Å²]
N1		1a	1		-3.16178	0.39223	-0.34356	0.0000
C2		1a	1		-3.88796	-0.00333	-0.31684	0.0000
C3		1a	1		-3.56742	0.27151	-0.34758	0.0000
C4		1a	1		-3.50889	0.31556	-0.33855	0.0000
C5		1a	1		-3.33270	0.30842	-0.36656	0.0000
C6		1a	1		-3.21849	0.25698	-0.40391	0.0000
C7		1a	1		-3.27722	0.21264	-0.41292	0.0000
C8		1a	1		-3.52421	0.19480	-0.22985	0.0000
C9		1a	1		-3.49876	0.23483	-0.19306	0.0000
C10		1a	1		-3.44990	0.28278	-0.17883	0.0000
C11		1a	1		-3.42412	0.29003	-0.20168	0.0000
C12		1a	1		-3.45038	0.24995	-0.23838	0.0000
C13		1a	1		-3.66250	-0.02560	-0.38030	0.0000
C14		1a	1		-3.72185	-0.06691	-0.38550	0.0000
C15		1a	1		-3.83853	-0.05514	-0.35224	0.0000
C16		1a	1		-3.82791	0.03664	-0.31293	0.0000
C17		1a	1		-3.71397	0.02654	-0.34409	0.0000
C18		1a	1		-3.50295	0.20152	-0.25338	0.0000
C19		1a	1		-3.44602	0.21922	-0.38466	0.0000
C20		1a	1		-3.61610	0.03869	-0.48022	0.0000
C21		1a	1		-3.64252	0.07141	-0.33728	0.0000
C22		1a	1		-3.59929	0.11476	-0.30196	0.0000
C23		1a	1		-3.53832	0.16046	-0.29056	0.0000
C24		1a	1		-3.52195	0.16261	-0.31681	0.0000
C25		1a	1		-3.46357	0.20670	-0.30794	0.0000
C26		1a	1		-3.45277	0.20938	-0.33311	0.0000
C27		1a	1		-3.65142	0.03454	-0.42446	0.0000
C28		1a	1		-3.66692	0.03200	-0.39907	0.0000
C29		1a	1		-3.62320	0.07362	-0.36334	0.0000
C30		1a	1		-3.56498	0.11934	-0.35306	0.0000
C31		1a	1		-3.52861	0.12818	-0.42957	0.0000
C32		1a	1		-3.57895	0.08176	-0.44116	0.0000
C33		1a	1		-3.59345	0.07890	-0.41532	0.0000
C34		1a	1		-3.55284	0.12207	-0.37906	0.0000
C35		1a	1		-3.50124	0.16813	-0.36857	0.0000
C36		1a	1		-3.49313	0.17159	-0.39394	0.0000
C37		1a	1		-3.49075	0.42849	-0.39141	0.0000
C38		1a	1		-3.38672	0.39800	-0.38443	0.0000
C39		1a	1		-3.28111	0.42164	-0.35166	0.0000
C40		1a	1		-3.28029	0.47535	-0.32629	0.0000
C41		1a	1		-3.38608	0.50568	-0.33309	0.0000
C42		1a	1		-3.49141	0.48277	-0.36564	0.0000
O43		1a	1		-4.00161	0.58319	-0.31476	0.0000
O44		1a	1		-3.20592	0.45118	-0.43032	0.0000
C45		1a	1		-3.42671	0.49662	-0.40522	0.0000
N46		1a	1		-3.59639	0.51516	-0.37214	0.0000
C47		1a	1		-3.84703	0.56673	-0.34383	0.0000
C48		1a	1		-3.92803	0.60305	-0.34803	0.0000
C49		1a	1		-4.17304	0.65578	-0.31901	0.0000
C50		1a	1		-3.31648	0.51551	-0.44245	0.0000
C51		1a	1		-3.50031	0.53248	-0.41002	0.0000
C52		1a	1		-3.74686	0.58521	-0.38088	0.0000
C53		1a	1		-3.24655	0.35102	-0.35609	0.0000
C54		1a	1		-3.61104	-0.01307	-0.49737	0.0000
C55		1a	1		-3.63861	-0.05266	-0.53414	0.0000
C56		1a	1		-3.67063	-0.04113	-0.55455	0.0000
C57		1a	1		-3.67609	0.01004	-0.53794	0.0000
C58		1a	1		-3.64960	0.04948	-0.50120	0.0000
C59		1a	1		-3.53782	0.54768	0.05449	0.0000
C60		1a	1		-3.50245	0.59278	0.09369	0.0000
C61		1a	1		-3.37661	0.57370	0.11104	0.0000
C62		1a	1		-3.54719	0.53181	0.10071	0.0000
C63		1a	1		-3.45837	0.48540	0.05856	0.0000
N64		1a	1		-3.49532	0.49547	0.03757	0.0000
C65		1a	1		-3.41626	0.51292	0.11787	0.0000
O66		1a	1		-3.35189	0.43881	0.04317	0.0000

O67	1a	1	-3.60657	0.55891	0.03784	0.0000
C68	1a	1	-3.48660	0.45149	-0.00197	0.0000
C69	1a	1	-3.58609	0.40620	-0.01586	0.0000
C70	1a	1	-3.57801	0.36408	-0.05361	0.0000
C71	1a	1	-3.47403	0.36644	-0.07842	0.0000
C72	1a	1	-3.37449	0.41126	-0.06510	0.0000
C73	1a	1	-3.37826	0.45290	-0.02747	0.0000
N74	1a	1	-3.48434	0.32396	-0.11657	0.0000
C75	1a	1	-3.43136	0.32627	-0.14012	0.0000
C76	1a	1	-3.68553	-0.08213	-0.59360	0.0000
C77	1a	1	-3.87898	-0.09641	-0.35463	0.0000
C78	1a	1	-4.09485	-0.28827	-0.35762	0.0000
C79	1a	1	-4.04844	-0.32617	-0.35475	0.0000
C80	1a	1	-3.80618	-0.37908	-0.38417	0.0000
C81	1a	1	-3.61629	-0.39604	-0.41642	0.0000
C82	1a	1	-3.66001	-0.35667	-0.41813	0.0000
N83	1a	1	-3.89202	-0.30381	-0.38849	0.0000
C84	1a	1	-3.37376	-0.44904	-0.44560	0.0000
O85	1a	1	-3.47867	-0.37101	-0.44546	0.0000
O86	1a	1	-4.31249	-0.24267	-0.33204	0.0000
C87	1a	1	-3.89897	-0.26335	-0.38792	0.0000
C88	1a	1	-3.90246	-0.27495	-0.41994	0.0000
C89	1a	1	-3.89244	-0.23588	-0.41908	0.0000
C90	1a	1	-3.88103	-0.18466	-0.38617	0.0000
C91	1a	1	-3.88065	-0.17302	-0.35419	0.0000
C92	1a	1	-3.88868	-0.21184	-0.35514	0.0000
N93	1a	1	-3.85659	-0.14548	-0.38575	0.0000
C94	1a	1	-3.40546	-0.35130	-0.78654	0.0000
C95	1a	1	-3.33063	-0.39780	-0.82850	0.0000
C96	1a	1	-3.41524	-0.37884	-0.84646	0.0000
C97	1a	1	-3.77499	-0.33344	-0.82450	0.0000
C98	1a	1	-3.78888	-0.28828	-0.78361	0.0000
N99	1a	1	-3.61957	-0.29900	-0.76603	0.0000
O100	1a	1	-3.96751	-0.24190	-0.76568	0.0000
O101	1a	1	-3.25909	-0.36080	-0.77100	0.0000
C102	1a	1	-3.65749	-0.25490	-0.72602	0.0000
C103	1a	1	-3.61960	-0.20539	-0.70999	0.0000
C104	1a	1	-3.64085	-0.16366	-0.67192	0.0000
C105	1a	1	-3.70040	-0.17058	-0.64892	0.0000
C106	1a	1	-3.74275	-0.21951	-0.66452	0.0000
C107	1a	1	-3.72294	-0.26124	-0.70270	0.0000
N108	1a	1	-3.70219	-0.12949	-0.61023	0.0000
C109	1a	1	-0.51500	-2.43902	-0.83963	0.0000
C110	1a	1	-0.82771	-2.31324	-0.84187	0.0000
C111	1a	1	-0.85294	-2.35903	-0.88162	0.0000
C112	1a	1	-1.23351	-2.30915	-1.32237	0.0000

Table S2: TGA and BET data of COFs based imine-imide linkage

COF	T_{d5} (°C)	T_{d10} (°C)	Char yield (wt%)	Surface area (m^2 g^{-1})	Average Pore size (nm)
Py-DNII-COF	481	522	55.22	183.00	4.10
TFPB-DNII-COF	502	524	38.00	45.00	7.30

Table S3. Thermodynamic parameters of four steps decomposition of COFs (a = Py-DNII-COF, b= TFPB-DNII-COF), where (Ts: setup decomposition temp.; E_a: activation energy; ΔS: entropy; ΔH: enthalpy, ΔG: Gibbs free energy)

COF	step	Start (°C)	End (°C)	Ts (°C)	E_a ($J.mol^{-1}$)	ΔS ($J.mol^{-1}.K^{-1}$)	ΔH ($J.mol^{-1}$)	ΔG ($J.mol^{-1}$)
a	1st	300	420	352	27386	-291.44	22189.86	204342
	2nd	421	521	515	87191	-206.15	80640.07	243084
	3rd	521	757	635	55274	-245.55	47725.05	270688
b	1st	450	593	546	142841	-131.26	136031.73	243530
	2nd	593	791	661	59570	-237.37	53018.39	240063

COFs	Band Gap (eV)	Metal Co-Catalyst	Sacrificial Element	HER Efficiency	Ref.
Py-DNII-COF	2.37	Pt	AA	625 µmol h^{-1} g^{-1}	This work
PTP-COF	2.1	Pt	TEOA	83.83 µmol h^{-1} g^{-1}	[4]
TP-EDDA **TP-BDDA**	2.34 2.31	Pt	TEOA	324 ± 10 µmol h^{-1} g^{-1} 30 ± 5 µmol h^{-1} g^{-1}	[5]
A(B/N/Y)PY-COF	1.94–1.92	Pt	TEOA	98 µmol h^{-1} g^{-1}	[6]
v-COF-NS1	1.85	Pt	AA	4.4 mmol h^{-1} g^{-1}	[7]
COF-BBT	2.0	Pt	AA	48.7 mmol g^{-1} h^{-1}	[8]
azine-linked N_2-COF	-	molecular cobaloxime	TEOA	782 µmol g^{-1} h^{-1}	[9]
TpDTz COF	2.07	NiME cluster	TEOA	941 µmol h^{-1} g^{-1}	[10]
pCOF10	-	cobaloxime catalyst	TEOA	163 µmol h^{-1} g^{-1}	[11]
TTR-COF	2.71	Au	TEOA	1720 µmol h^{-1} g^{-1}	[12]
MoS_2/TpPa-1-COF	2.14	MoS_2	AA	55.85 µmol h^{-1}	[13]
BT-TAPT-COF	2.35	Pt	TEOA	949 µmol g^{-1} h^{-1}	[14]
Py-ClTP-BT-COF	2.36	Pt	AA	177.50 µmol h^{-1} g^{-1}	[15]
NKCOF-108	1.8	Pt	AA	120 µmol h^{-1}	[16]
BtCOF150	2.5	Pt	TEOA	750 ± 25 µmol h^{-1} g^{-1}	[17]
PTPA-COF **TP-COF**	2.31 2.41	Pt	TEOA	36 µmol h^{-1} g^{-1} 29.12 mmol h^{-1} g^{-1}	[18]
TAPFy-PhI COF	2.21	Pt	AA	1763 µmol g^{-1} h^{-1}	[19]
TpPa−COF−$(CH_3)_2$	2.06	Pt	NaAA	8033 µmol g^{-1} h^{-1}	[20]
PyPz-COF	2.05	Pt	AA	7542 µmol g^{-1} h^{-1}	[21]

Table S4: Comparison of HER values of Py-DNII-COF with other COF based materials.

References

1 Y. Li, L. Guo, Y. Lv, Z. Zhao, Y. Ma, W. Chen, G. Xing, D. Jiang and L. Chen, *Angew. Chemie Int. Ed.*, 2021, **60**, 5363–5369.

2 L. Ascherl, E. W. Evans, M. Hennemann, D. Di Nuzzo, A. G. Hufnagel, M. Beetz, R. H. Friend, T. Clark, T. Bein and F. Auras, *Nat. Commun.*, 2018, **9**, 3802.

3 S. P. Black, D. M. Wood, F. B. Schwarz, T. K. Ronson, J. J. Holstein, A. R. Stefankiewicz, C. A. Schalley, J. K. M. Sanders and J. R. Nitschke, *Chem. Sci.*, 2016, **7**, 2614–2620.

4 F. Haase, T. Banerjee, G. Savasci, C. Ochsenfeld and B. V Lotsch, *Faraday Discuss.*, 2017, **201**, 247–264.

5 P. Pachfule, A. Acharjya, J. Roeser, T. Langenhahn, M. Schwarze, R. Schomäcker, A. Thomas and J. Schmidt, *J. Am. Chem. Soc.*, 2018, **140**, 1423–1427.

6 L. Stegbauer, S. Zech, G. Savasci, T. Banerjee, F. Podjaski, K. Schwinghammer, C. Ochsenfeld and B. V Lotsch, *Adv. Energy Mater.*, 2018, **8**, 1870107.

7 S. Li, R. Ma, S. Xu, T. Zheng, H. Wang, G. Fu, H. Yang, Y. Hou, Z. Liao and B. Wu, *ACS Catal.*, 2023, **13**, 1089–1096.

8 W. Huang, Y. Hu, Z. Qin, Y. Ji, X. Zhao, Y. Wu, Q. He, Y. Li, C. Zhang and J. Lu, *Natl. Sci. Rev.*, 2023, **10**, nwac171.

9 V. Artero, M. Chavarot-Kerlidou and M. Fontecave, *Angew. Chemie Int. Ed.*, 2011, **50**, 7238–7266.

10 B. P. Biswal, H. A. Vignolo-González, T. Banerjee, L. Grunenberg, G. Savasci, K. Gottschling, J. Nuss, C. Ochsenfeld and B. V Lotsch, *J. Am. Chem. Soc.*, 2019, **141**, 11082–11092.

11 K. Gottschling, G. Savasci, H. Vignolo-González, S. Schmidt, P. Mauker, T. Banerjee, P. Rovó, C. Ochsenfeld and B. V Lotsch, *J. Am. Chem. Soc.*, 2020, **142**, 12146–12156.

12 L. Li, Z. Zhou, L. Li, Z. Zhuang, J. Bi, J. Chen, Y. Yu and J. Yu, *ACS Sustain. Chem. Eng.*, 2019, **7**, 18574–18581.

13 M.-Y. Gao, C.-C. Li, H.-L. Tang, X.-J. Sun, H. Dong and F.-M. Zhang, *J. Mater. Chem. A*, 2019, **7**, 20193–20200.

14 G.-B. Wang, S. Li, C.-X. Yan, Q.-Q. Lin, F.-C. Zhu, Y. Geng and Y.-B. Dong, *Chem. Commun.*, 2020, **56**, 12612–12615.

15 W. Chen, L. Wang, D. Mo, F. He, Z. Wen, X. Wu, H. Xu and L. Chen, *Angew. Chemie*, 2020, **132**, 17050–17057.

16 Z. Zhao, Y. Zheng, C. Wang, S. Zhang, J. Song, Y. Li, S. Ma, P. Cheng, Z. Zhang and Y. Chen, *ACS Catal.*, 2021, **11**, 2098–2107.

17 S. Ghosh, A. Nakada, M. A. Springer, T. Kawaguchi, K. Suzuki, H. Kaji, I. Baburin, A. Kuc, T. Heine and H. Suzuki, *J. Am. Chem. Soc.*, 2020, **142**, 9752–9762.

18 H. Liu, D. Wang, Z. Yu, Y. Chen, X. Li, R. Zhang, X. Chen, L. Wu, N. Ding and Y. Wang, *Sci. China Mater.*, 2023, 1–7.

19 G. Zhang, M. Zhao, L. Su, H. Yu, C. Wang, D. Sun and Y. Ding, *ACS Appl. Mater. Interfaces*, 2023, **15**, 20310–20316.

20 J. Sheng, H. Dong, X. Meng, H. Tang, Y. Yao, D. Liu, L. Bai, F. Zhang, J. Wei and X. Sun, *ChemCatChem*, 2019, **11**, 2313–2319.

21 F. Wang, L. Yang, X. Wang, Y. Rong, L. Yang, C. Zhang, F. Yan and Q. Wang, *Small*, 2023, 2207421.